PHYSICAL REVIEW C **84**, 011301(R) (2011)

Emergence of the $N = 16$ shell gap in ^{21}O

B. Fernández-Domínguez,[1,2,3] J. S. Thomas,[4] W. N. Catford,[4] F. Delaunay,[3] S. M. Brown,[4] N. A. Orr,[3] M. Rejmund,[2] M. Labiche,[5] M. Chartier,[1] N. L. Achouri,[3] H. Al Falou,[3] N. I. Ashwood,[6] D. Beaumel,[7] Y. Blumenfeld,[7] B. A. Brown,[8] R. Chapman,[9] N. Curtis,[6] C. Force,[2] G. de France,[2] S. Franchoo,[7] J. Guillot,[7] P. Haigh,[6] F. Hammache,[7] V. Lapoux,[10] R. C. Lemmon,[5] F. Maréchal,[7] A. M. Moro,[11] X. Mougeot,[10] B. Mouginot,[7] L. Nalpas,[10] A. Navin,[2] N. Patterson,[4] B. Pietras,[1] E. C. Pollacco,[10] A. Leprince,[3] A. Ramus,[7] J. A. Scarpaci,[7] N. de Séréville,[7] I. Stephan,[7] O. Sorlin,[2] and G. L. Wilson[4]

[1]*Oliver Lodge Laboratory, University of Liverpool, Liverpool L69 7ZE, United Kingdom*

[2]*Grand Accélérateur National d'Ions Lourds, BP 55076, 14076 Caen Cedex 5, France*

[3]*Laboratoire de Physique Corpusculaire de Caen, École Nationale Supérieure d'Ingénieurs de Caen, Université de Caen, Centre National de la Recherche Scientifique et Institute National de Physique Nucléaire et de Physique des Particules, 14050 Caen Cedex, France*

[4]*Department of Physics, University of Surrey, Guildford GU2 5XH, United Kingdom*

[5]*Nuclear Physics Group, STFC Daresbury Laboratory, Daresbury, Warrington WA4 4AD, United Kingdom*

[6]*School of Physics and Astronomy, University of Birmingham, Birmingham B15 2TT, United Kingdom*

[7]*Institut de Physique Nucléaire, Institute National de Physique Nucléaire et de Physique des Particles and Centre National de la Recherche Scientifique, 91406 Orsay Cedex, France*

[8]*National Superconducting Cyclotron Laboratory, Michigan State University East Lansing, Michigan 48824-1321, USA*

[9]*SUPA, School of Science and Engineering, University of the West of Scotland, Paisley, PA1 2BE, United Kingdom*

[10]*Commissariat à l'Énergie, Centre de Saclay, Institut de Recherche sur les lois Fondamentales de l'Univers, Service de Physique Nucléaire, F-91191 Gif-sur-Yvette, France*

[11]*Departamento de Física Atómica, Molecular y Nuclear, Universidad de Sevilla, E-41080 Sevilla, Spain*

(Received 5 April 2011; published 6 July 2011; publisher error corrected 28 July 2011)

The spectroscopy of ^{21}O has been investigated using a radioactive ^{20}O beam and the (d,p) reaction in inverse kinematics. The ground and first excited states have been determined to be $J^\pi = 5/2^+$ and $1/2^+$, respectively. Two neutron unbound states were observed at excitation energies of 4.77(10) and 6.17(11) MeV. The spectroscopic factor deduced for the lower of these, interpreted as a $3/2^+$ level, reveals a relatively pure (60%) $0d_{3/2}$ single-particle configuration, in good agreement with shell-model calculations that predict ^{26}O to be unbound. The large energy difference between the $3/2^+$ and $1/2^+$ states is indicative of the emergence of the $N = 16$ shell gap, which is estimated to be 5.1(11) MeV. For the higher-lying resonance, which has a character consistent with a spin-parity assignment of $3/2^+$ or $7/2^-$, a 0.71(22) branching ratio to the first 2^+ state in ^{20}O has been observed.

DOI: 10.1103/PhysRevC.84.011301 PACS number(s): 25.60.Je, 21.60.Cs, 21.10.Jx, 23.20.Lv

The magic numbers that explain the structure of nuclei close to stability have their origin in the gaps created by the single-particle eigenstates of the mean field. The structure of nuclei far from stability is now known to generally differ, exhibiting an evolution of the shell closures or even a reordering of the levels [1]. The single-particle properties can be modified in light neutron-rich nuclei by the combined action of the central component and the tensor part of the effective nucleon-nucleon (NN) interaction [2,3]. Furthermore, near the drip line, other effects become important including many-body correlations [4–6] and the influence of the scattering to the continuum [7–9].

The neutron-rich oxygen isotopes represent an intriguing region to study the interplay of such effects. The last bound oxygen isotope is ^{24}O, which reinforces $N = 16$ as a shell gap, but the addition of a single proton moves the neutron-drip line for the fluorine isotopes to ^{31}F ($N = 22$) [10]. The $N = 16$ gap is produced by an increase in the spacing between the $1s_{1/2}$ and the $0d_{3/2}$ neutron orbitals. Precise knowledge of how the energy of these orbitals evolve is crucial in order to predict the position of the neutron-drip line and the properties of nuclei lying beyond it. The $N = 16$ gap is predicted to open up at low Z and to be clearly developed in the oxygen isotopes [11–13]. This is evident in both the USD [11] and SDPF-M [13] interactions, but the size of the gap is significantly larger in the latter. The only experimental estimates of this gap[1] are provided by a measurement in ^{23}O using the ^{22}O(d,p) transfer reaction [14] [4.00(2) MeV], which favors the USDA interaction (a modified version of the USD interaction) [12], and a measurement of the ground state in ^{25}O [15] [4.86(13) MeV], which agrees with the USD calculations, which predict ^{26}O to be bound, in contradiction to experiment [16]. In fact, the size of the $N = 16$ gap depends relatively weakly on the neutron number [11–13], so it is possible to gain more in-depth information by investigating a more readily accessible nucleus such as ^{21}O. In addition, the $N = 14$ gap has previously been inferred from inelastic proton scattering on ^{22}O [17] to be 3.2(2) MeV, but also has had no independent verification.

Here we have employed the $d(^{20}\mathrm{O},p\gamma)$ reaction as a means to shed light on the evolution of the $\nu 0d_{3/2}$ strength and infer the size of the $N = 14$ and 16 gaps. Multinucleon transfer [18] and in-beam γ-ray spectroscopy following fragmentation [19]

[1]An accurate measure of the gap requires a full mapping of the $0d_{3/2}$ and $0s_{1/2}$ strengths [33].

provide evidence for a low-lying $3/2^+$ state ($E_x = 2.13$ MeV) in ^{21}O, but this is expected to include significant core excitation rather than a strong $\nu 0d_{3/2}$ single-particle structure [18]. We report here on the observation of a higher-lying neutron unbound $3/2^+$ level that carries significant $\nu 0d_{3/2}$ strength. In addition, a second unbound level was observed. While a definitive spin-parity assignment could not be made, the observation of neutron decay to the first excited 2^+ state of ^{20}O indicates a considerable core-excited component.

The experiment was performed at the SPIRAL facility using a 10.5-A MeV ^{20}O beam with an integrated intensity of 1.65×10^9 particles and a typical rate of 10^4 particles per second. The target was a 0.59-mg/cm^2-thick CD_2 foil. The (d,p) reaction channel was selected using the identification of the beamlike residue in the VAMOS spectrometer and the kinematics of the proton, as measured using the TIARA silicon array [20] from 36° to 169° in the laboratory frame. The excitation energy in ^{21}O and the c.m. scattering angle were obtained from the measured energy and angle of the recoiling protons. The bound first excited state of ^{21}O was determined to lie at 1.21(4) MeV. As in our earlier work [20,21], the target was also surrounded at 90° by four EXOGAM clover detectors in a close-packed geometry (photopeak efficiency, including addback [20], of 10(1)% at 800 keV). The coincident γ rays indicated an excitation energy of 1.213(7) MeV. Both values compare well with the most precise previous measurement of 1.218(4) MeV [19] (Table I). A detailed description of the experimental setup can be found in Refs. [20–22].

The excitation energy spectrum deduced for states lying above the neutron emission threshold ($S_n = 3.81(1)$ MeV [23]) in ^{21}O is shown in Fig. 1. The solid line represents the sum of two resonances (dashed lines) and a contribution from direct breakup ($^{20}\mathrm{O} + n + p$). The resonance line shape employed was a Breit-Wigner distribution convoluted with a Gaussian of fixed width (full width at half maximum $\mathrm{FWHM_{exp}}$) that represented the experimental resolution arising from the beam characteristics (spot size and energy spread), the energy and angular straggling in the target, detector resolutions, and kinematic effects. The three-body contribution was obtained by uniformly sampling the simulated phase space of such a decay and applying the same geometric cuts as used to treat the data. The normalization was determined in the high-excitation-energy region of the spectrum. A Monte Carlo simulation [20] based on GEANT4 was employed to determine the experimental resolution. The simulation was validated by comparison with the measured resolution of the state at

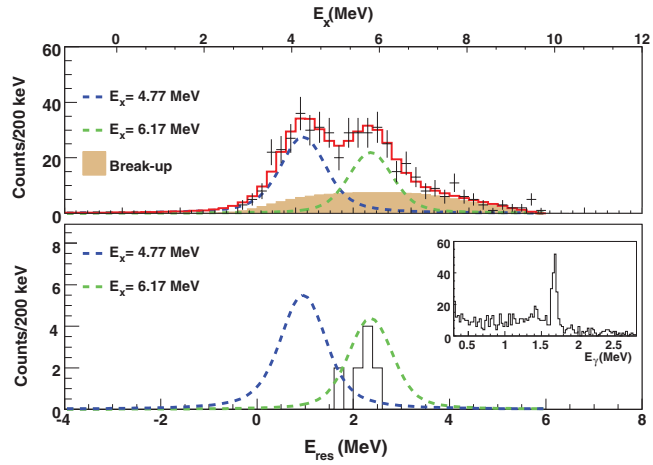

FIG. 1. (Color online) Upper panel: Excitation energy spectrum of the unbound states in ^{21}O from $^{20}\mathrm{O} + p$ coincidences, including the contribution from direct breakup (see the text). Lower panel: Spectrum for $^{20}\mathrm{O} + p$ events in coincidence with 1684-keV deexcitation γ rays from $^{20}\mathrm{O}(2_1{}^+)$. For comparison the 4.77 and 6.17 resonances are shown after renormalization. The inset shows the Doppler-corrected γ-ray spectrum gated on ^{20}O and requiring that a light particle be recorded in TIARA.

1.21 MeV: $\mathrm{FWHM_{exp}} = 0.77(17)$ MeV and $\mathrm{FWHM_{sim}} = 0.75$ MeV. The simulation was then used to estimate the resolution at higher excitation energies. The adjustment to the data yielded energies and widths for the resonances of $E_{\mathrm{res}_1} = 0.96(10)$, $\Gamma_1 = 0.46(20)$ and $E_{\mathrm{res}_2} = 2.36(11)$, $\Gamma_2 = 0.32(26)$ MeV. The corresponding excitation energies are 4.77(10) and 6.17(11) MeV.

The lower panel of Fig. 1 displays the excitation-energy spectrum for $^{20}\mathrm{O} + p + \gamma$ triple coincidences for the 1.684-MeV photopeak events. It is clear, despite the somewhat limited statistics, that part of the strength for the neutron decay of the 6.17-MeV resonance proceeds to the 1.684-MeV 2^+ first excited state of ^{20}O. Taking into account the Lorentz boosted γ-ray detection efficiency (6.4%), the branching ratio for this decay path was determined to be $\Gamma(2^+)/\Gamma_{\mathrm{tot}} = 0.71(22)$, where the uncertainty is dominated by the statistics.

Elastic scattering was used to calibrate the product of the beam current and the number of deuterons in the target. Figure 2 displays the angular distributions for the protons leading to the bound and unbound states in ^{21}O compared to reaction model calculations. The theoretical cross

TABLE I. Results from the present work for ^{21}O. The excitation energies and spin-parity assignments are compared with those of earlier studies using multinucleon transfer [18], in-beam γ-ray spectroscopy following fragmentation [19], and neutron knockout [30]. Tentative spin-parity assignments are noted within parentheses.

E_x (keV) present	E_x (keV) [18]	E_x (keV) [19]	ℓ present	J^π present	J^π [18]	J^π [19]	J^π [30]	C^2S present
0	0	0	2	$5/2^+$	$(5/2^+)$	$(5/2^+)$	$5/2^+$	0.34 ± 0.08
1213 ± 7	1330 ± 90	1218 ± 4	0	$1/2^+$	$(1/2^+)$	$(1/2^+)$		0.77 ± 0.19
4770 ± 100			2	$3/2^+$				0.58 ± 0.14
6170 ± 110			2,3	$(3/2^+,7/2^-)$				$(0.30 \pm 0.07, 0.20 \pm 0.05)$

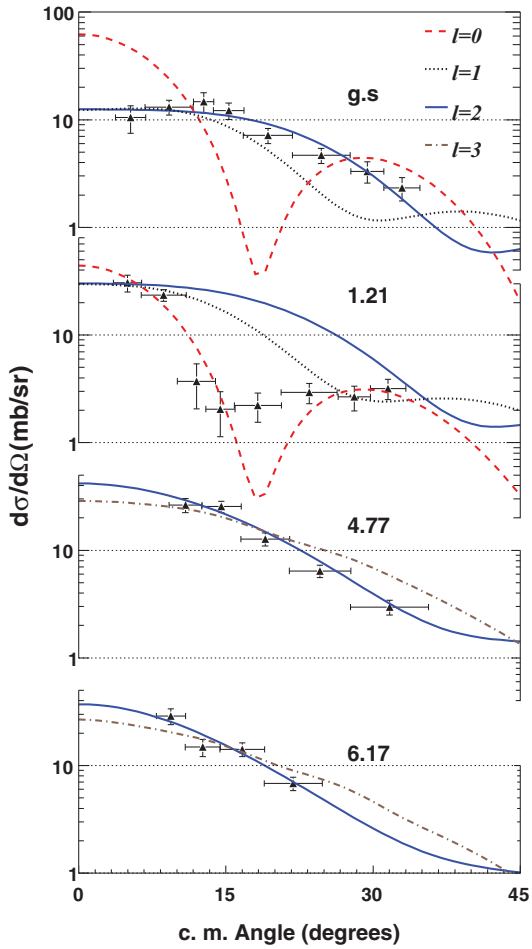

FIG. 2. (Color online) Differential cross sections for the states populated in ^{21}O compared to adiabatic distorted-wave approximation calculations. Only statistical uncertainties are included.

sections were computed within the adiabatic distorted-wave approximation using an adiabatic potential for the $d + ^{20}$O entrance channel [24]. The Chapel-Hill parameterisation (CH89) [25] was used to describe the nucleon-nucleus potentials for both the entrance and outgoing channels. The calculations for the unbound states were performed using the Vincent-Fortune prescription [26] implemented in DWUCK4 [27]. The neutron single-particle form factors were obtained using a Woods-Saxon potential with the depth adjusted to reproduce the experimental binding energy of each level. The results for the unbound states were cross-checked using bins to represent each resonance in the continuum within the FRESCO code [28]. Consistent results for the angular distributions were obtained with the two approaches. The uncertainties in the spectroscopic factors (C^2S) arising from statistics, the normalization, and the minimization procedure are approximately 15%. The final uncertainties, including a reaction model contribution estimated to be 20% [29], are 25%. Table I summarizes the present results and includes a comparison, where available, with earlier work.

The angular distribution for the transfer to the ground state is well reproduced by an $\ell = 2$ transfer, consistent with the $5/2^+$ assignment derived from neutron knockout [30] and proposed by other studies [18,19]. The differential cross sections for the 1.21-MeV state are consistent only with an $\ell = 0$ transfer, which permits a definite $1/2^+$ assignment to this state. The spectroscopic factors were obtained by minimizing the χ^2 for all the data points. The spectroscopic factors for the ground and first excited states were determined to be 0.34(8) and 0.77(19), respectively, in agreement with shell-model calculations using the USDA, SDPF-M, and WBP [31] (USD for the *sd* shell) interactions (Fig. 3). The $5/2^+$ and $1/2^+$ bound states carry most of the available strength of the $0d_{5/2}$ and $1s_{1/2}$ orbitals, respectively, based on the vacancies in ^{20}O. The $1s_{1/2}$ strength is smaller than unity owing to this orbital being partially occupied in the projectile. This is consistent with a complementary study we have carried out of the ^{20}O(d,t) ^{19}O reaction in which the lowest $1/2^+$ state in ^{19}O was populated [22].

Turning to the unbound states, it may be noted that the widths strongly suggest $\ell \geqslant 2$ assignments, as the single-particle widths for $\ell = 1$ are very broad (e.g., $\Gamma_{sp} \approx 4$ MeV at $E_{res} = 1$ MeV). The angular distribution for the resonant state at $E_x = 4.77$ MeV is best reproduced by an $\ell = 2$ transition, which would imply $J^\pi = (3/2^+, 5/2^+)$. As the $\nu 0d_{5/2}$ strength was exhausted in the ground state by sum rule considerations the state at 4.77 MeV is therefore assigned to be $3/2^+$. The corresponding experimental spectroscopic factor of 0.58(14) is in good agreement with the USDA value of 0.68 for the $3/2_2{}^+$ state, while, as shown in Fig. 3, the WBP interaction predicts this state to carry a somewhat larger fraction of the $0d_{3/2}$ single-particle strength. The SDPF-M interaction predicts the $3/2_2{}^+$ state to have a very low spectroscopic factor and the strength is instead concentrated in the $3/2_3{}^+$ state.

For the second unbound state at 6.17 MeV, the angular distribution for $\ell = 2$ gives the best fit to the data but $\ell = 3$ cannot be excluded, owing to a more limited angular range in the measurements.[2] The corresponding spectroscopic factors are 0.30(7) and 0.20(5), respectively. From Fig. 3, the states expected to be strongly populated in the (d,p) reaction can be identified. Leaving aside the $3/2_2{}^+$ state (the $3/2_3{}^+$ state in the SDPF-M interaction) identified with the 4.77-MeV state, the remaining candidates are the other $3/2^+$ states together with the $7/2^-$ states. The only states in Fig. 3 favoring decay to ^{20}O$(2_1{}^+)$ turn out to be the $3/2_3{}^+(3/2_4{}^+$ state in the SDPF-M interaction) and the $7/2_2{}^-$ states. For these $3/2^+$ states, the three interactions predict values of 0.69, 0.74, and 0.76 for $\Gamma(2^+)/\Gamma_{tot}$, but the (d,p) spectroscopic factor in each case is only 0.1 (Fig. 3). If it were assumed that the state at 6.17 MeV has $J^\pi = 3/2^+$, then the $0d_{3/2}$ strength would be split between the 4.77- and 6.17-MeV states in a manner that is not predicted by the calculations. The other possibility is a $7/2^-$ assignment, with a wave function carrying a small part of the $\nu 0f_{7/2}$ strength and dominated by core excitations coupled to a $\nu 1p_{3/2}$ neutron. Ideally, coupled-channel calculations should be carried out. While beyond the scope of the present work, exploratory calculations suggest that the utility of any

[2]The energies of the protons with $\theta_{c.m.} \geqslant 30^\circ$ were below the detection threshold.

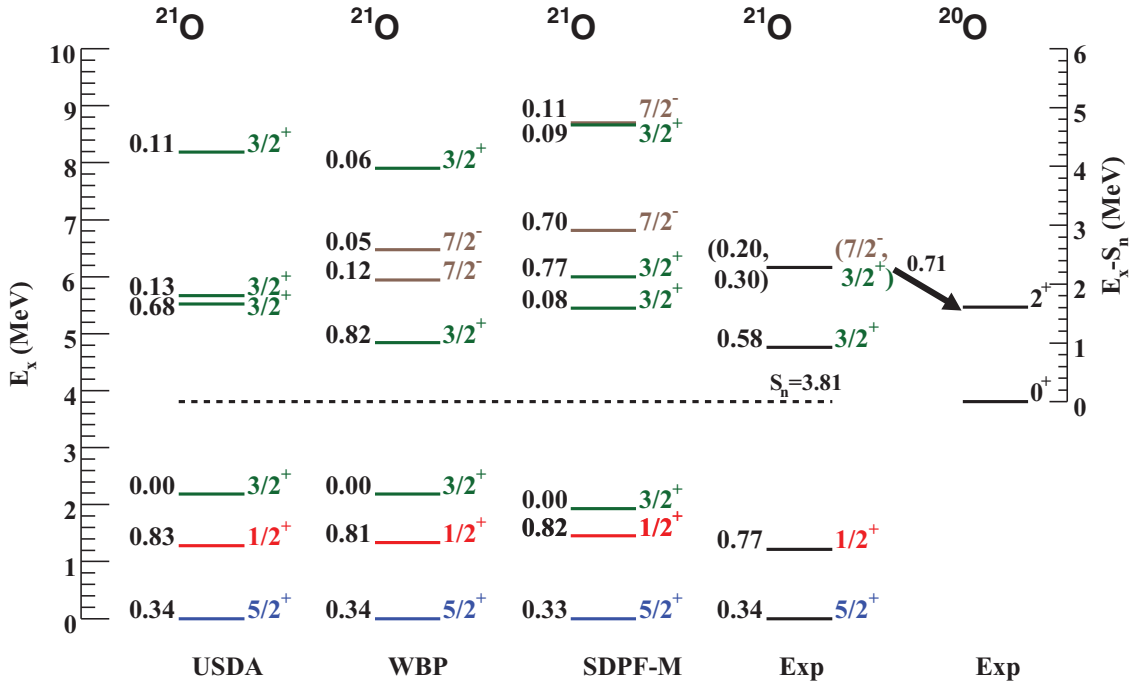

FIG. 3. (Color online) Results from the present work for the states observed in ^{21}O compared to shell-model calculations. For clarity only states of relevance to the present study are shown. The numbers on the left-hand side of levels correspond to the spectroscopic factors. The experimental uncertainties are listed in Table I.

such effort would be limited owing to the restricted angular range of the present data.

An estimate of the lower limit of the size of the $N = 16$ shell gap in ^{21}O can be deduced from the difference in excitation energies of the $1/2^+$ [$E_x = 1.21(1)$ MeV] and the $3/2^+$ [$E_x = 4.77(10)$ MeV] states. The value here of 3.55(10) MeV is close to the estimate of 4.00(2) MeV in ^{23}O deduced in the same manner [14]. The equivalent value for ^{25}O is 4.86(13) MeV [15]. By using the more complete formalism of Refs. [32,33] and incorporating the corresponding uncertainties in E_x and C^2S, the neutron single-particle energies ϵ can be derived for ^{20}O. This requires the C^2S for neutron removal from ^{20}O, which were obtained in parallel with the present measurement through the $d(^{20}\mathrm{O},t)\,^{19}\mathrm{O}$ reaction [34]. The results are $\epsilon 0d_{5/2} = -6.47(171)$ MeV, $\epsilon 1s_{1/2} = -4.18(100)$ MeV, and $\epsilon 0d_{3/2} = 0.95(36)$ MeV. The calculations assume that all (d,t) and (d,p) strengths have been measured experimentally for the $0d_{5/2}$ and $1s_{1/2}$ orbitals. The value for $\epsilon 0d_{3/2}$ represents a lower limit. We note that the corresponding shell gaps $\nu 1s_{1/2} - \nu 0d_{5/2} = 2.29(198)$ MeV ($N = 14$) and $\nu 0d_{3/2} - \nu 1s_{1/2} = 5.13(106)$ ($N = 16$) are consistent with the effective single-particle energies of the USDA and USDB interactions [12].

In summary, the results for neutron transfer onto ^{20}O populating states in ^{21}O have been presented. The first excited state was assigned spin parity $1/2^+$ and the $\ell = 2$ transfer to the ground state supports a $5/2^+$ assignment. The spectroscopic factors derived for both states are in good agreement with the shell-model predictions. Two neutron unbound states have also been observed at 4.77 and 6.17 MeV. The 4.77-MeV state is identified as $3/2^+$ and carries approximately 60% of the $\nu 0d_{3/2}$ strength. The spectroscopic factor agrees with the USDA interaction calculations that correctly predict ^{26}O to be unbound. The $N = 16$ shell gap was thus estimated to be 5.1(11) MeV, which is somewhat larger than the lower limit of 3.55(10) MeV derived from the energy difference between the $3/2^+$ resonance and the $1/2^+$ level. The state at 6.17 MeV, which was observed to decay predominantly to $^{20}\mathrm{O}(2_1{}^+)$, corresponds either to a large fraction of the missing $\nu 0d_{3/2}$ strength or to an intruder $\nu 0f_{7/2}$ state from the pf shell. The shell model is unable to provide an adequate explanation for this level. This poses a challenge for it and the interactions used to describe the evolution of nuclear structure in this region. Ideally, the issues discussed here should be investigated using models that include explicitly the effects of the continuum. Finally, it has been shown experimentally that triple coincidence fragment-particle-γ measurements can be of utility in investigating the structure of unbound states through their decay. This suggests that future nucleon transfer experiments exploring states in the continuum should incorporate highly efficient γ-ray arrays.

The authors acknowledge the excellent support provided by the technical staff of Laboratoire de Physique Corpusculaire de Caen and Grand Accélérateur National d'Ions Lourds and wish to thank Dr. N. Timofeyuk and Professor J. Camacho, Professor J.A. Tostevin, and Professor Y. Utsuno for fruitful discussions. This work was supported in part by the European Union Sixth Framework through the EURISOL Design-Study Contract No. 515768 RIDS and by the National Science Foundation Grant No. PHY-0758099.

[1] O. Sorlin and M.-G. Porquet, Prog. Part. Nucl. Phys. **61**, 602 (2008).
[2] N. A. Smirnova *et al.*, Phys. Lett. B **686**, 109 (2010).
[3] T. Otsuka *et al.*, Phys. Rev. Lett. **104**, 012501 (2010).
[4] T. Otsuka, T. Suzuki, J. D. Holt, A. Schwenk, and Y. Akaishi, Phys. Rev. Lett. **105**, 032501 (2010).
[5] G. Hagen, T. Papenbrock, D. J. Dean, M. Hjorth-Jensen, and B. Velamur Asokan, Phys. Rev. C **80**, 021306 (2009).
[6] G. Hagen, T. Papenbrock, D. J. Dean, and M. Hjorth-Jensen, Phys. Rev. C **82**, 034330 (2010).
[7] J. Dobaczewski *et al.*, Prog. Part. Nucl. Phys. **59**, 432 (2007).
[8] K. Tsukiyama, M. Hjorth-Jensen, and G. Hagen, Phys. Rev. C **80**, 051301 (2009).
[9] N. Michel *et al.*, Nucl. Phys. A **794**, 29 (2007).
[10] H. Sakurai *et al.*, Phys. Lett. B **448**, 180 (1999).
[11] http://www.nscl.msu.edu/∼brown/resources/SDE.HTM
[12] B. A. Brown and W. A. Richter, Phys. Rev. C **74**, 034315 (2006).
[13] Y. Utsuno, T. Otsuka, T. Mizusaki, and M. Honma, Phys. Rev. C **60**, 054315 (1999).
[14] Z. Elekes *et al.*, Phys. Rev. Lett. **98**, 102502 (2007).
[15] C. R. Hoffman *et al.*, Phys. Rev. Lett. **100**, 152502 (2008).
[16] M. Fauerbach *et al.*, Phys. Rev. C **53**, 647 (1996); D. Guillemaud-Mueller *et al.*, *ibid.* **41**, 937 (1990).
[17] C. R. Hoffman *et al.*, Phys. Rev. Lett. **100**, 152502 (2008).
[18] W. N. Catford *et al.*, Nucl. Phys. A **503**, 263 (1989).
[19] M. Stanoiu *et al.*, Phys. Rev. C **69**, 034312 (2004).
[20] M. Labiche *et al.*, Nucl. Instrum. Methods A **614**, 439 (2010).
[21] W. N. Catford *et al.*, Phys. Rev. Lett. **104**, 192501 (2010).
[22] A. Ramus *et al.*, Int. J. Mod. Phys. E **18**, 1 (2009).
[23] G. Audi *et al.*, Nucl. Phys. A **729**, 337 (2003).
[24] R. C. Johnson and P. C. Tandy, Nucl. Phys. A **235**, 56 (1974).
[25] R. L. Varner *et al.*, Phys. Rep. **201**, 57 (1991).
[26] C. M. Vincent and H. T. Fortune, Phys. Rev. C **2**, 782 (1970).
[27] P. D. Kunz, http://spot.colorado.edu/∼kunz/DWBA.html
[28] I. J. Thompson, Comput. Phys. Rep. **7**, 167 (1988).
[29] J. Lee, M. B. Tsang, and W. G. Lynch, Phys. Rev. C **75**, 064320 (2007).
[30] E. Sauvan *et al.*, Phys. Lett. B **491**, 1 (2000); Phys. Rev. C **69**, 044603 (2004).
[31] E. K. Warburton and B. A. Brown, Phys. Rev. C **46**, 923 (1992).
[32] M. Baranger, Nucl. Phys. A **149**, 225 (1970).
[33] A. Signoracci and B. A. Brown, Phys. Rev. Lett. **99**, 099201 (2007).
[34] A. Ramus, Ph.D. thesis, Université de Paris XI, 2009 [http://tel.archives-ouvertes.fr/docs/00/45/75/09/PDF/TheseRamus.pdf].